

Evaluation of *p*-phenylene-bis and phenyl dithiocarbamate sodium salts as inhibitors of mushroom tyrosinase

Ehsan Amin¹, Ali Akbar Saboury¹✉, Hassan Mansouri-Torshizi², Samane Zolghadri¹ and Abdol-Khalegh Bordbar³

¹Institute of Biochemistry and Biophysics, University of Tehran, Tehran, Iran; ²Department of Chemistry, University of Sistan & Bluchestan, Zahedan, Iran; ³Department of Chemistry, University of Isfahan, Isfahan, Iran

Two structurally related compounds, phenyl dithiocarbamate sodium salt (I) and *p*-phenylene-bis (dithiocarbamate) sodium salt (II) were prepared by reaction of the parent aniline and *p*-phenylenediamine with CS₂ in the presence of sodium hydroxide. These water soluble compounds were characterized by spectroscopic techniques, IR, ¹H NMR and elemental analysis. The inhibitory effects of both compounds on both activities of mushroom tyrosinase (MT) from *Agaricus bisporus* were studied at two temperatures, 27°C and 37°C. L-3, 4-dihydroxyphenylalanine (L-DOPA), and L-tyrosine were used as natural substrates for the catecholase and cresolase enzyme reactions, respectively. Kinetic analysis confirmed noncompetitive inhibition mode of I and mixed type of II on both activities of MT; I and II inhibit MT with inhibition constants (*K_i*) of 300 μM and 4 μM, respectively. Analysis of thermodynamic parameters indicated predominant involvement of hydrophobic interactions in binding of I and electrostatic ones in binding of II to MT. It seems that II is a more potent MT inhibitor due to its two charged head groups able to chelate copper ions in the enzyme active site. Intrinsic fluorescence studies as a function of concentrations of both compounds showed unexpectedly quenching of emission intensity without any shift of emission maximum. Extrinsic ANS-fluorescence indicated that only binding of I induces limited changes in the tertiary structure of MT, in agreement with the postulated hydrophobic nature of the binding mechanism.

Keywords: mushroom tyrosinase, *p*-phenylene-bis (dithiocarbamate), phenyl dithiocarbamate, noncompetitive inhibition, mixed inhibition, inhibition constant

Received: 19 August, 2010; revised: 09 June, 2010; accepted: 08 July, 2010; available on-line: 19 August, 2010

INTRODUCTION

Tyrosinase (polyphenol oxidase EC 1.14.18.1) is a copper-containing enzyme (Matoba *et al.*, 2006) involved in pigment biosynthesis of various organisms. Mushroom tyrosinase (MT) from *Agaricus bisporus* due to its accessibility is well characterized and has been used in enzymatic studies (Nakamura *et al.*, 1966; Jolley & Nelson, 1969). It has been proposed that MT consists of two subunits, a heavy (H) and a light (L) with molecular mass of 43 kDa and 13.4 kDa, respectively. In aqueous solution the predominant form of MT has the quaternary structure (HL)₂ with an estimated molecular mass of 120 kDa (Strothkamp *et al.*, 1976). The active site of

tyrosinase consists of two closely spaced copper ions each coordinated by three histidine residues (Decker *et al.*, 2006). The two Cu(II) ions are coupled antiferromagnetically (Holm *et al.*, 1996). This copper pair is the site of interaction of tyrosinase with both molecular oxygen and its organic substrates. In this active site, mono-oxygenation of monophenols to diphenols (cresolase activity) and oxidation of diphenols to *o*-quinones (catecholase activity) are catalyzed (Fenoll *et al.*, 2001).

In fruits, fungi and vegetables the melanins are responsible for the formation of melanins leading to browning of wounded tissue exposed to air and the browning occurring during post-harvest storage (Fraignier *et al.*, 1995; Garcia-Molina *et al.*, 2005; Halaoui *et al.*, 2006). In agriculture, browning poses a significant problem of huge economical impact (Artes *et al.*, 1998; Seo *et al.*, 2003; Bittner, 2006). The accumulation of an abnormal melanin amount in different specific parts of the skin, resulting in more pigmented patches, is also an esthetic problem. Tyrosinase inhibition is the most common approach to achieve skin depigmentation (Briganti *et al.*, 2003; Parvez *et al.*, 2006). Therefore, identification of compounds that inhibit melanin formation is extremely important. A considerable number of tyrosinase inhibitors are known (Kim & Uyama, 2005). Synthetic tyrosinase inhibitors may be used as drugs and chemicals (captopril and methimazole) (Espin & Wichers, 2001). Much effort has been put into searching for effective tyrosinase inhibitors because of their broad applications. In the last decades, thiol compounds have been extensively investigated as tyrosinase inhibitors, among them alkylidenethiosemicarbazide, *n*-alkyl xanthates, *n*-alkyl dithiocarbamates, *N*-aryl *S*-alkylthiocarbamate, phenylthiourea, and tetrathiotungstate (Gheibi *et al.*, 2005; Lee *et al.*, 2005; Park *et al.*, 2006; Aljanianzadeh & Saboury, 2007; Aljanianzadeh *et al.*, 2007; Criton & Mellay-Hammon, 2008; Liu *et al.*, 2009).

Dithiocarbamates are organosulfur compounds of robust synthetic and chemical properties (Siddiqi *et al.*, 2007) and are produced in great quantities (Vaneet *et al.*, 2005; Khwaja *et al.*, 2006). Their insecticidal, herbicidal, and fungicidal properties, have a wide range of applications. Because of their high biological activity, dithiocarbamates are also used in medicine, the rubber industry, and in the treatment of chronic alcoholism (Givsepina *et al.*, 2005). The chemical properties of dithiocar-

✉ e-mail: saboury@ut.ac.ir

Abbreviations: ANS, 1-anilinonaphthalene-8-sulfonate; L-DOPA, 4-dihydroxyphenylalanine; MT, mushroom tyrosinase

bamates are due to the presence of one or more active –NCSS– group in their structures. This functional group can form complexes with almost all elements, including metal atoms of metal-containing enzymes, thus blocking their catalytic activity (Sanchez-Cortes *et al.*, 1998). More recently, our group has studied the inhibitory effects of some synthetic thiocarbamates on mushroom tyrosinase activities (Gheibi *et al.*, 2005; Saboury *et al.*, 2006; 2007; Alijanianzadeh & Saboury, 2007; Alijanianzadeh *et al.*, 2007; Amin *et al.*, 2009). In the present investigation, a kinetic analysis is presented of the inhibition of both cresolase and catecholase activities by *p*-phenylene-bis and phenyl dithiocarbamate sodium salts (Fig. 1) at two temperatures.

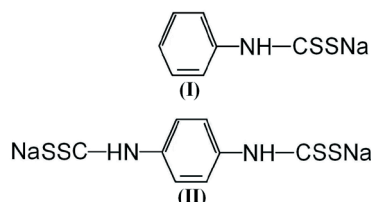


Figure 1. Structure of phenyl dithiocarbamate sodium salt (I) and *p*-phenylene-bis(dithiocarbamate) sodium salt (II)

MATERIALS AND METHODS

Materials. Mushroom tyrosinase (MT; EC 1.14.18.1; specific activity 5370 units/mg), L-3, 4-dihydroxyphenylalanine (L-DOPA), L-tyrosine and 1-anilino-naphthalene-8-sulfonate (ANS) were purchased from Sigma. CS₂, NaOH, aniline and *p*-phenylenediamine were used as supplied (Aldrich products). The solvents used were purchased from Merck Chemical Company. Phosphate buffer (50 mM, pH 6.8) was used throughout this work. All buffers were prepared with water purified by a Milli Q water purification system.

Methods. Infrared spectra in KBr pellets were recorded on a Nicolet 5-DXB FT-IR spectrophotometer in the range of 4000–400 cm⁻¹. ¹H NMR spectra in DMSO-d₆ were recorded on a Bruker DRX-500 Avance spectrophotometer at 500 MHz using sodium-3-trimethylpropionate as the internal reference. ¹H NMR data are expressed in parts per million (ppm) and are reported as chemical shift position (δH), multiplicity (s = singlet, d = doublet, t = triplet, q = quartet, m = multiplet, sb = singlet broad) and assignment. Melting points were measured on a unimelt capillary melting point apparatus and are reported uncorrected. Microchemical analysis of carbon, hydrogen and nitrogen were carried out on CHN Rapid Heraeus.

Synthesis of phenyl dithiocarbamate sodium salt, NaSSC–HN–C₆H₅ (I). This compound was prepared by a modified literature method (Desai *et al.*, 2006; Manav *et al.*, 2006). Aniline (4.55 mL, 50 mmol) solved in acetone (40 mL) and sodium hydroxide (2 g, 50 mmol) solved in double distilled water (20 mL) were mixed and stirred vigorously in an ice bath. CS₂ (10 mL, excess) was added dropwise. Stirring continued for one hour in an ice bath and another three hours at room temperature. The mixture was then filtered, the volume of filtrate was reduced on a Rota evaporator to complete dryness and washed with acetone.

This crude product was recrystallized by dissolving in 50 mL acetone and filtering the undissolved particles out. Dichloromethane (50 mL) was added to the filtrate and placed in a refrigerator overnight. The desired product

I (yield 8.20 g, 85%) was collected by filtration as white crystalline powder and washed with a small amount of dichloromethane and vacuum dried. Analysis (calculated for C₇H₆NS₂Na): C, 43.98; H, 3.14; N, 7.33%; found: C, 43.97; H, 3.15; N, 7.31%. Solid-state IR spectroscopy of **I** showed two characteristic bands at 1480 cm⁻¹ and 969 cm⁻¹ assigned to ν(N-CSS) and ν(SCS) modes, respectively (Givseppina *et al.*, 2005). ¹H NMR (500 MHz, DMSO-d₆, ppm): 6.88 (m, a *para* = CH-), 7.14 (m, two *meta* = CH-), 7.86 (m, two *ortho* = CH-), 10.01 (sb, -NH-).

Synthesis of *p*-phenylene-bis(dithiocarbamate) sodium salt, NaSSC–NH–C₆H₄–NH–CSSNa (II).

The same procedure as for **I** was applied. To a solution of *p*-phenylenediamine (5.41 g, 50 mmol) in acetone (40 mL) was added 40 mL of aqueous solution of sodium hydroxide (4 g, 100 mmol), and the mixture was stirred and cooled to 0°C. To the cold mixture 10 mL (excess) of CS₂ was added dropwise under vigorous stirring. The yellow solution so obtained was stirred for 2 h at 0°C and 12 h at room temp. It was then filtered and the filtrate evaporated under reduced pressure nearly to dryness. Over the yellow viscous liquid so obtained 30 mL of acetone was poured and the mixture stirred until the product of reaction solidified into the yellow powder. It was filtered and dissolved in 40 mL of water and filtered again. Acetone (80 mL) was added to the filtrate and left in a refrigerator overnight. The desired product was collected by filtration as white crystals, washed with acetone and vacuum dried. Yield was 12.92 g (85%). Analysis (calculated for C₈H₆N₂S₄Na₂): C, 31.58; H, 1.97; N, 9.21% found C, 31.56; H, 1.96; N, 9.22%. Solid-state IR spectroscopy of **II** showed two characteristic bands at 1494 and 971 cm⁻¹ assigned to ν(N-CSS) and ν(SCS) modes, respectively (Givseppina *et al.*, 2005). ¹H NMR (500 MHz, DMSO-d₆, ppm): 7.61 (s, -C₆H₄-), 9.83 (sb, -NH-).

Kinetic measurements. Kinetic assays of mushroom tyrosinase were determined by measuring spectrophotometrically at 475 nm (A₄₇₅ the amount of dopachrome formed in the reaction mixture using a Cary spectrophotometer 100 Biomodel, with jacketed cell holders) (García-Molina *et al.*, 2007). First the enzyme dissolved in one milliliter of 50 mM phosphate buffer (pH 6.8) was incubated with different concentrations of each inhibitor. Then, the substrate was added to the reaction mixture and the reaction was monitored for 2 min. The final concentration of MT was 26.07 µg/mL for the cresolase activity and 6.52 µg/mL for the catecholase activity. The measurement was performed in triplicate for each experiment and averaged before further calculation. The inhibitory effects of both compounds were determined at two temperatures: 27°C and 37°C. For estimation of the type of inhibition and obtain K_i values, the experimental results were analysed by Lineweaver-Burk plots.

Intrinsic and ANS-binding fluorescence experiments. The fluorescence emission spectra were measured with a Hitachi spectrofluorimeter, MPF-4 model, equipped with a thermostatically controlled cuvette compartment. The tryptophan fluorescence was excited at 280 nm. The changes of the extrinsic fluorescence intensity were studied by labeling MT with ANS, at the molar concentration ratio of

$$\frac{C_{ANS}}{C_{Enzyme}} = 50$$

for 10 min prior to measurement (Gasyimov & Glasgow, 2007). The fluorescence of bound ANS was excited at 390 nm.

RESULTS AND DISCUSSION

For evaluating the inhibitory activity of the two compounds (**I** and **II**) tyrosinase inhibition assays were performed using L-tyrosine and L-DOPA as cresolase and catecholase substrates of the enzyme, respectively. In order to obtain thermodynamic parameters, the experiments were carried out at two temperatures: 27°C and 37°C.

Inhibitory effects of **I** on MT activities

In the cresolase activity assay, after about 15 s (lag time) the curve of absorbance (A_{475}) versus time rose nearly linearly, with a constant slope, referred to as the initial steady state rate. In the catecholase activity assay the steady state rate was reached without a lag time. The steady state rate of the two activities decreased with increasing concentration of compound **I**. The Lineweaver-Burk equation, which can be used to determine the type of inhibition, is:

$$\frac{1}{V} = \frac{K'_m}{V'_{\max}} \frac{1}{S} + \frac{1}{V'_{\max}} \quad (1)$$

where V and V'_{\max} are the initial and maximum velocities, respectively, and K'_m is the Michaelis-Menten constant in the presence of an inhibitor. The Lineweaver-Burk plots of $1/V$ vs. $1/[S]$ in the presence and absence of an inhibitor may be used to determine the type of inhibition (Saboury, 2009). These plots in the absence and presence of a noncompetitive inhibitor at different fixed concentrations intersect each other on the X-axis, which means that the inhibitor does not change the K'_m while V'_{\max} is gradually decreased (Figs. 2–5). The type of the slope and/or vertical intercept (Y-int) dependence on the inhibitor concentration can also be used to determine the inhibition constant (K_i) according to a plot named the secondary plot (insets in Figs. 2–5):

$$Y - \text{int} = \frac{1}{V_{\max}} \left(1 + \frac{[I]}{K_i} \right) \quad (2)$$

So, considering Lineweaver-Burk plots at different concentrations of **I**, shown in Figs. 2–5, we can conclude that in both temperatures compound **I** inhibits MT noncompetitively. Also, inhibition constants of **I** were calculated from the insets in figures and summarized in Table 1. The understanding of molecular recognition processes of ligand binding to biological macromolecules requires complete characterization of the binding energetic. A quantitative description of the forces that govern molecular associations requires determination of changes of all thermodynamic parameters, including standard free energy (ΔG°), enthalpy (ΔH°), and entropy (ΔS°) of binding (Perozzo *et al.*, 2004). ΔG° can be calculated from association constant as follows:

$$\Delta G^\circ = -RT \ln K_a \quad (3)$$

where R is the gas constant and T is the absolute temperature. Also, ΔH° may be obtained from association constants K_{a1} and K_{a2} ($K_{a2} = 1/K_i$) in two temperatures of T_1 and T_2 , respectively, using van't Hoff equation:

$$\ln \frac{K_{a2}}{K_{a1}} = -\frac{\Delta H^\circ}{R} \left(\frac{1}{T_2} - \frac{1}{T_1} \right) \quad (4)$$

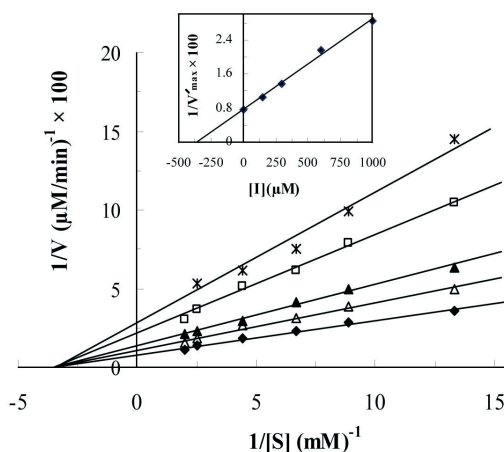


Figure 2. Lineweaver-Burk plots in the presence of fixed concentrations of **I** for cresolase reactions; Inset: $1/V_{\max}$ versus inhibitor concentration [**I**]

L-Tyrosine was a substrate. The assay was done in 50 mM sodium phosphate buffer, pH 6.8, at 27°C and 26.07 μg/mL enzyme, in the presence of different concentrations of **I**: 0 μM (◆), 150 μM (△), 300 μM (▲), 600 μM (□), 1000 μM (*).

Finally, ΔS° is directly calculated from ΔG° and ΔH° according to Eqn. 5:

$$\Delta S^\circ = \frac{(\Delta H^\circ - \Delta G^\circ)}{T} \quad (5)$$

All thermodynamic parameters of **I** binding are summarized in Table 1. In noncompetitive inhibition, both **I** and the substrate bind to different sites of the enzyme independently. The degree of inhibition is unaffected by changes in the substrate concentration. The negative ΔG° value indicates spontaneous binding of **I** to MT. Also, the decrease of dissociation constant following with increase temperature indicates that binding is entropy driven.

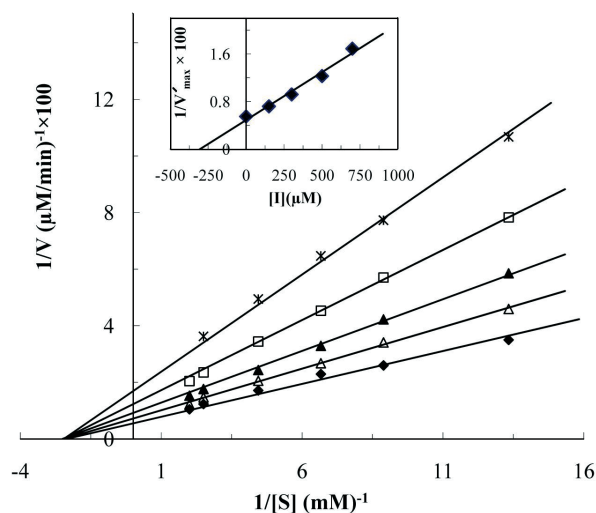


Figure 3. Lineweaver-Burk plots in the presence of fixed concentrations of **I** for cresolase reactions; Inset: $1/V_{\max}$ versus inhibitor concentration [**I**]

L-Tyrosine was a substrate. The assay was done in 50 mM sodium phosphate buffer, pH 6.8, at 37°C and 26.07 μg/mL enzyme, in the presence of different concentrations of **I**: 0 μM (◆), 150 μM (△), 300 μM (▲), 600 μM (□), 1000 μM (*).

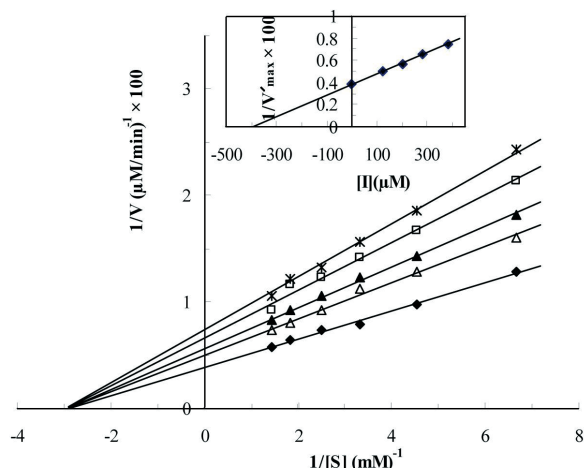


Figure 4. Lineweaver-Burk plots in the presence of fixed concentrations of **I** for catecholase activities; Inset: $1/V_{\max}$ versus inhibitor concentration $[I]$

L-DOPA was a substrate. The assay was done in 50 mM sodium phosphate buffer, pH 6.8, at 27°C and 6.52 μg/mL enzyme, in the presence of different concentrations of **I**: 0 μM (◆), 120 μM (△), 200 μM (▲), 280 μM (□), 380 μM (*).

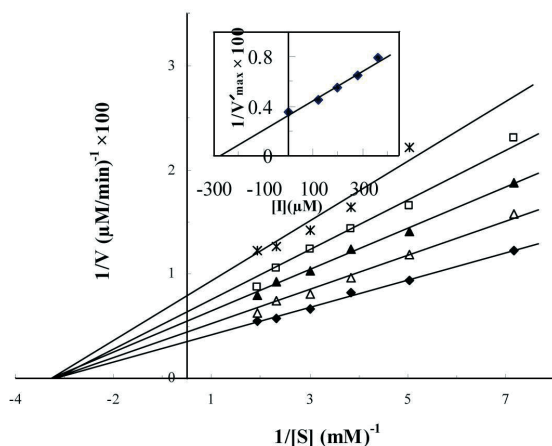


Figure 5. Lineweaver-Burk plots in the presence of fixed concentrations of **I** for catecholase activities; Inset: $1/V_{\max}$ versus inhibitor concentration $[I]$.

L-DOPA was a substrate. The assay was done in 50 mM sodium phosphate buffer, pH 6.8, at 37°C and 6.52 μg/mL enzyme, in the presence of different concentrations of **I**: 0 μM (◆), 120 μM (△), 200 μM (▲), 280 μM (□), 380 μM (*).

en and that hydrophobic forces are predominant ones in the mechanism of binding. On the other hand, many compounds containing sulfur atoms are known as metal ions chelating agents and competitive inhibitors of MT

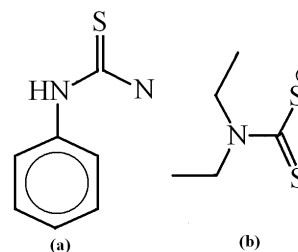


Figure 6. (a) Phenylthiourea, (b) Diethylthiocarbamate.

catalytic activity (Rescigno *et al.*, 2002; Gheibi *et al.*, 2005; Ronconi *et al.*, 2005). Chelating of ions involves electrostatic forces. So, the hydrophobic tail of compound **I** (Fig. 1) it is likely to play a considerable role both in binding as well as in chelating by its dithiol head of a copper ion in the active site of MT. Furthermore, similar results were reported before. Diethylthiocarbamate was shown to act as a competitive inhibitor while phenylthiourea as a noncompetitive one (Fig. 6) (Rescigno *et al.*, 2002; Criton & Mellay-Hamon, 2008). The greater entropy change accompanying catecholase activity than that of cresolase one show that hydrophobic interactions play a very important role in the catecholase activity.

Inhibitory effects of **II** on MT activities

In fixed concentrations of compound **II** and different concentration of each of the two substrates, initial steady state rates of enzymatic reactions were measured at two temperatures for both activities. The results thus obtained are shown in the form of Lineweaver-Burk plots in Figs. 7–10. The Lineweaver-Burk plots (Eqn. 1) in the absence and presence of a mixed type inhibitor at its different fixed concentrations may intersect each other above the negative X-axis which means that both K_m and V_{\max} change as a function of the concentration of this inhibitor type (Saboury, 2009). Also the slope and Y-int vary as follows:

$$Y - \text{int} = \frac{1}{V_{\max}} \left[1 + \frac{[I]}{\alpha K_I} \right] \quad (6)$$

$$\text{Slope} = \frac{K_m}{V_{\max}} \left[1 + \frac{[I]}{K_I} \right] \quad (7)$$

where α is the interaction parameter for binding sites of substrate and inhibitor and K_I is the inhibition constant of equilibrium binding of inhibitor to the enzyme (*E*). So, by plotting secondary plots (insets in Figs. 7–10) one can calculate K_I values (summarized in Table 2). Also, the inhibition constants in two temperatures were used to obtain thermodynamic parameters (Table 2). This results

showed that compound **II** can bind not only to the free enzyme but also to the enzyme–substrate complex and thereby decreasing the affinity of the substrate. The increasing K_I values with increasing temperature indicates that the binding is enthalpy driven and consequently, involves predominantly electrostatic forces. Considering the chemical structure of compound **II** (Fig. 1) and the thermodynamics of its binding to MT it seems that **II** with two

Table 1. Inhibition and thermodynamic parameters of binding of phenyl dithiocarbamate sodium salt (**I**) to MT

Reaction type	Temperature (°C)	K_I (μM)	K_3 (M ⁻¹)	ΔG° (kJ mol ⁻¹)	ΔH° (kJ mol ⁻¹)	$T\Delta S^\circ$ (kJ mol ⁻¹)
Cresolase	27	361	2770	-20	12	32
	37	307	3257	-21		33
Catecholase	27	380	2632	-20	26	46
	37	270	3704	-21		47

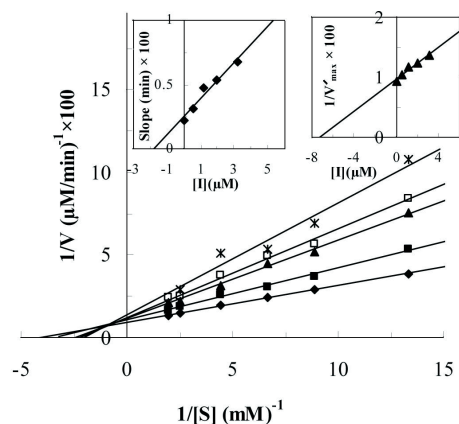


Figure 7. Lineweaver-Burk plots in the presence of fixed concentrations of **II** for cresolase activities; Insets: slope and $1/V_{\max}$ of Lineweaver-Burk plots versus inhibitor concentrations [**II**]. L-tyrosine was a substrate. The assay was done in 50 mM sodium phosphate buffer, pH 6.8, at 27°C and 26.07 μg/mL enzyme, in the presence of different concentrations of **II**: 0 μM (◆), 0.6 μM (■), 1.2 μM (▲), 2 μM (□), 3.2 μM (*).

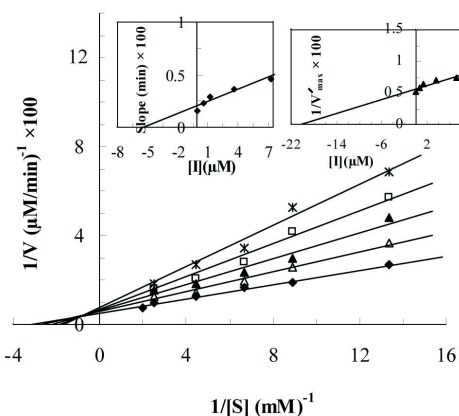


Figure 8. Lineweaver-Burk plots in the presence of fixed concentrations of **II** for cresolase activities; Insets: slope and $1/V_{\max}$ of Lineweaver-Burk plots versus inhibitor concentrations [**II**]. L-tyrosine was a substrate. The assay was done in 50 mM sodium phosphate buffer, pH 6.8, at 37°C and 26.07 μg/mL enzyme, in the presence of different concentrations of **II**: 0 μM (◆), 0.6 μM (Δ), 1.2 μM (▲), 3.6 μM (□), 7.2 μM (*).

negatively charged heads can chelate copper ions in the enzyme active site and thus affect the binding affinity of the substrate. Compound **II** is apparently a more potent inhibitor than **I**, in agreement with the notion that electrostatic forces play a very important role in the inhibition of MT by thiol compounds.

Table 2. Inhibition and thermodynamic parameters of binding of *p*-phenylene-bis (dithiocarbamate) sodium salt (**II**) to MT

Reaction type	Temperature (°C)	K_i (μM)	α	K_s ($M^{-1} \times 10^5$)	ΔG° (kJ mol ⁻¹)	ΔH° (kJ mol ⁻¹)	$T\Delta S^\circ$ (kJ mol ⁻¹)
Cresolase	27	1.8	4.2	5.56	-33	-85	-52
	37	5.3	3.9	1.89	-31		-42
Catecholase	27	1.7	4.6	5.88	-33	-128	-94
	37	9	5.5	1.11	-30		-98

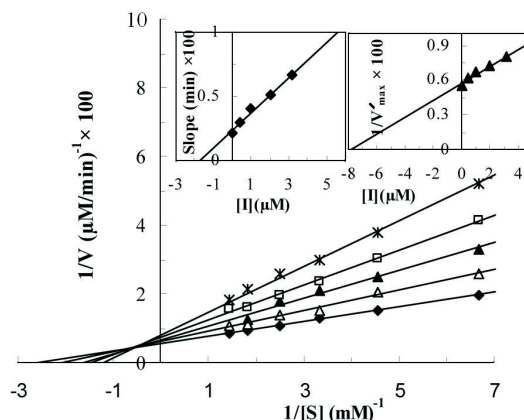


Figure 9. Lineweaver-Burk plots in the presence of fixed concentrations of **II** for catecholase activities; Insets: slope and $1/V_{\max}$ of Lineweaver-Burk plots versus inhibitor concentrations [**II**]. L-DOPA was a substrate. The assay was done in 50 mM sodium phosphate buffer, pH 6.8, at 27°C and 6.52 μg/mL enzyme, in the presence of different concentrations of **II**: 0 μM (◆), 0.4 μM (Δ), 1.0 μM (▲), 2.0 μM (□), 3.2 μM (*).

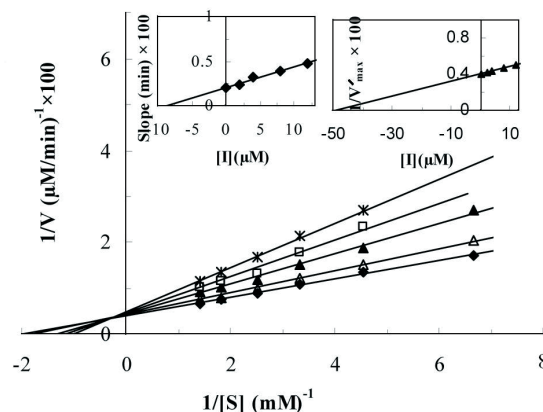


Figure 10. Lineweaver-Burk plots in the presence of fixed concentrations of **II** for catecholase activities; Insets: slope and $1/V_{\max}$ of Lineweaver-Burk plots versus inhibitor concentrations [**II**]. L-DOPA was a substrate. The assay was done in 50 mM sodium phosphate buffer, pH 6.8, at 37°C and 6.52 μg/mL enzyme, in the presence of different concentrations of **II**: 0 μM (◆), 2.0 μM (Δ), 4.0 μM (▲), 8.0 μM (□), 12.0 μM (*).

Fluorescence study

Intrinsic fluorescence of MT in the presence of **I** and **II** was measured in order to obtain additional information on the nature of their inhibitory effect on MT. Unexpectedly, addition of either of the two compounds to MT caused quenching of tryptophan emission (Fig. 11). It must be stressed that this quenching occurred without any change in the fluorescence band position. These observations suggest that no considerable conformational changes accompany binding of **I**

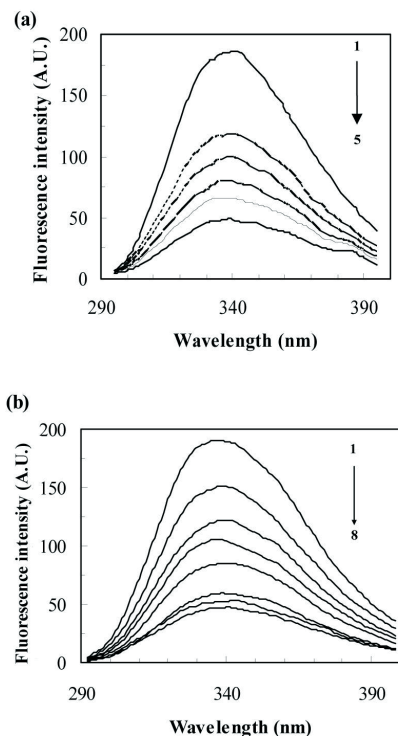


Figure 11. Intrinsic fluorescence changes of MT in the presence of different concentrations of (a) **I** and (b) **II**

The fluorescence emission spectra were measured in 50 mM sodium phosphate buffer, pH 6.8, at 27°C and 170 µg/mL enzyme, in the presence of different concentrations of **I** (1 to 5: 0, 80, 120, 180, 240, 320 µM) and **II** (1 to 8: 0, 0.2, 0.4, 0.8, 1.2, 2, 2.5, 3.2 µM). Wavelength of 280 nm was used to excite tryptophan residues of MT.

and **II**. Changes in extrinsic fluorescence of ANS upon its binding to MT in the presence of the two inhibitors were also monitored (Fig. 12). Only binding of **I** caused slight changes in ANS emission. This observation may indicate induction of minor changes in the tertiary structure of MT, incurred by hydrophobic interactions of the inhibitor with the enzyme.

CONCLUSION

The reported investigation documents effects of sodium salts of a monofunctional (**I**) and a bifunctional (**II**) dithiocarbamate on the activities and structure of mushroom tyrosinase. We hypothesize that the charged thiol heads of the dithiocarbamates play a direct role in the inhibition of tyrosinase by chelating the copper ions in its active site. Also, the phenolic group of **I** is suggested to interact with hydrophobic patches in the active site, thereby driving slight changes in the tertiary enzyme structure. It seems that these hydrophobic interactions decrease the inhibitory effects of the compound. On the other hand, the two charged heads of compound **II** interact electrostatically with the active site copper ions which diminishes its hydrophobic interaction. Compound **II** binds the active site of MT more strongly than **I** thereby decreasing the affinity of the substrate to the enzyme. This makes it an effective competitive inhibitor. Taking together, bifunctional dithiocarbamates, being strong chelators of copper ions, are potent tyrosinase inhibitors.

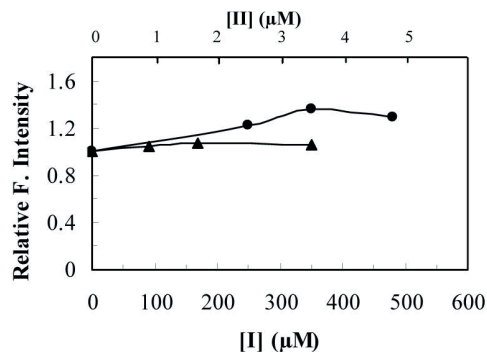


Figure 12. ANS-binding fluorescence spectra changes in the presence of various concentrations of **I** (lower axis: ●) and **II** (upper axis: ▲)

The fluorescence emission spectra were measured in 50 mM sodium phosphate buffer, pH 6.8, at 27°C. Excitation wavelength of 385 nm was used to detect the ANS fluorescence. Molar concentration ratio (ANS /MT) is 50.

Acknowledgements

The financial support given by the University of Tehran is gratefully acknowledged.

REFERENCES

- Alijanianzadeh M, Saboury AA (2007) Temperature dependence of activation and inhibition of mushroom tyrosinase by ethyl xanthate. *Bull Korean Chem Soc* **28**: 758–762.
- Alijanianzadeh M, Saboury AA, Mansuri-Torshizi H, Haghbeen K, Moosavi-Movahedi AA (2007) The inhibitory effect of some new synthesized xanthates on mushroom tyrosinase activities. *J Enzyme Inhib Med Chem* **22**: 239–246.
- Amin E, Saboury AA, Mansoori-Torshizi H, Moosavi-Movahedi AA (2009) Potent inhibitory effects of benzyl and *p*-xylylidine-bis dithiocarbamate sodium salts on activities of mushroom tyrosinase. *J Enzyme Inhib Med Chem* (In press).
- Artes F, Castaner M, Gil MI (1998) Review: Enzymatic browning in minimally processed fruit and vegetables. *Food Sci Technol Int* **4**: 377–389.
- Bittner S (2006) When quinones meet amino acids: chemical, physical and biological consequences. *Amino Acids* **30**: 205–224.
- Briganti S, Camera E, Picardo M (2003) Chemical and instrumental approaches to treat hyperpigmentation. *Pigment Cell Res* **16**: 101–110.
- Criton M, Mellay-Hamon VL (2008) Analogues of *N*-hydroxy-*N'*-phenylthiourea and *N*-hydroxy-*N'*-phenylurea as inhibitors of tyrosinase and melanin formation. *Bioorg Med Chem Lett* **18**: 3607–3610.
- Decker H, Schweikardt T, Tuzcek F (2006) The first crystal structure of tyrosinase: All questions answered? *Angew Chem Int Ed* **45**: 4546–4550.
- Desai RM, Shah MK, Shah VH (2006) Preparation and antimicrobial screening of Cu(II), Ni(II), Zn(II) and Cd(II) complexes. *Eur J Chem* **3**: 137–141.
- Espin JC, Wichers HJ (2001) Effect of captopril on mushroom tyrosinase activity *in vitro*. *Biochim Biophys Acta* **1544**: 289–300.
- Fenoll LG, Rodríguez-López JN, García-Sevilla F, García-Ruiz PA, Varón R, García-Canovas F, Tudela J (2001) Analysis and interpretation of the action mechanism of mushroom tyrosinase on monophenols and diphenols generating highly unstable *o*-quinones. *Biochim Biophys Acta* **1548**: 1–22.
- Fraignier MP, Marques L, Fleuriet A, Macheix JJ (1995) Biochemical and immunochemical characteristics of polyphenol oxidases from different fruits of Prunus. *J Agric Food Chem* **43**: 2375–2380.
- García-Molina F, Hiner AN, Fenoll LG, Rodríguez-López JN, García-Ruiz PA, García-Canovas F, Tudela J (2005) Mushroom tyrosinase: catalase activity, inhibition, and suicide inactivation. *J Agric Food Chem* **53**: 3702–3709.
- García-Molina F, Muñoz JL, Varón R, Rodríguez-López JN, García-Canovas F, Tudela J (2007) A review on spectrophotometric methods for measuring the monophenolase and diphenolase activities of tyrosinase. *J Agric Food Chem* **55**: 9739–9749.
- Gasymov OK, Glasgow BJ (2007) ANS fluorescence: potential to augment the identification of the external binding sites of proteins. *Biochim Biophys Acta* **1774**: 403–411.

- Gheibi N, Saboury AA, Mansuri-Torshizi H, Haghbeen K, Moosavi-Movahedi AA (2005) The inhibition effect of some *n*-alkyl dithiocarbamates on mushroom tyrosinase. *J Enzyme Inhib Med Chem* **20**: 393–399.
- Givseppina F, Sergio S, Diego M (2005) Pyrrolidine dithiocarbamates of Pd(II). *Inorg Chim Acta* **358**: 971–980.
- Halaoui S, Asther M, Sigoillot JC, Hamdi M, Lomascolo A (2006) Fungal tyrosinases: new prospects in molecular characteristics, bio-engineering and biotechnological applications. *J Appl Microbiol* **100**: 219–232.
- Holm RH, Kennepohl P, Solomon EI (1996) Structural and functional aspects of metal sites in biology. *Chem Rev* **96**: 2239–2314.
- Jolley RL, Nelson RM (1969) The multiple forms of mushroom tyrosinase. structural studies on the isoenzymes. *Biol Chem Hoppe-Seyler* **244**: 3251–3257.
- Khawaja SS, Shahab AAN, Lutfullah C, Yonas C (2006) Template synthesis of symmetrical transition metal dithiocarbamates. *J Barç Chem Soc* **17**: 107–112.
- Kim YJ, Uyama H (2005) Tyrosinase inhibitors from natural and synthetic sources: structure, inhibition mechanism and perspective for the future. *Cell Mol Life Sci* **62**: 1707–1723.
- Lee KH, Koketsu M, Choi SY, Lee KJ, Lee P, Ishihara H, Kim SY (2005) Potent inhibitory effects of *N*-aryl *S*-alkylthiocarbamate derivatives on the Dopa oxidase activity of mushroom tyrosinase. *Chem Pharm Bull (Tokyo)* **53**: 747–749.
- Liu J, Cao R, Yi W, Ma C, Wan Y, Zhou B, Ma L, Song H (2009) A class of potent tyrosinase inhibitors: alkylidenethiosemicarbazide compounds. *Eur J Med Chem* **44**: 1773–1778.
- Manav N, Mishra AK, Kaushik NK (2006) *In vitro* antitumour and antibacterial studies of some Pt(IV) dithiocarbamate complexes. *Spectrochim Acta Part A* **65**: 32–35.
- Matoba Y, Kumagai T, Yamamoto A, Yoshitsu H, Sugiyama M (2006) Crystallographic evidence that the dinuclear copper center of tyrosinase is flexible during catalysis. *J Biol Chem* **281**: 8981–8990.
- Nakamura T, Sho S, Ogura Y (1966) On the purification and properties of mushroom tyrosinase. *J Biochem* **59**: 481–486.
- Park KH, Lee JR, Hahn HS, Kim YH, Bae CD, Yang JM, Oh S, Bae YJ, Kim DE, Hahn M-J (2006) Inhibitory effect of ammonium tetrathiotungstate on tyrosinase and its kinetic mechanism. *Chem Pharm Bull (Tokyo)* **54**: 1266–1270.
- Parvez S, Kang M, Chung HS, Cho C, Hong MC, Shin MK, Bae H (2006) Survey and mechanism of skin depigmenting and lightening agents. *Phytother Res* **20**: 921–934.
- Perozzo R, Folkers G, Scapozza L (2004) Thermodynamics of protein–ligand interactions: history, presence, and future aspects. *J Recept Signal Transduct* **24**: 1–52.
- Rescigno A, Sollai F, Pisu B, Rinaldi A, Sanjust E (2002) Tyrosinase inhibition: General and applied aspects. *J Enzyme Inhib Med Chem* **17**: 207–218.
- Ronconi L, Maccato C, Barreca D, Saini R, Zancato MDF (2005) Gold (III) dithiocarbamate derivatives of *N*-methylglycine: an experimental and theoretical investigation. *Polyhedron* **24**: 521–531.
- Saboury AA, Alijanianzadeh M, Mansoori-Torshizi H (2007) The role of alkyl chain length in the inhibitory effect *n*-alkyl xanthates on mushroom tyrosinase activities. *Acta Biochim Pol* **54**: 183–191.
- Saboury AA (2009) Enzyme inhibition and activation: a general theory. *J Iran Chem Soc* **6**: 219–229.
- Saboury AA, Zolghadri S, Haghbeen K, Moosavi-Movahedi AA (2006) The inhibitory effect of benzenethiol on the cresolase and catecholase activities of mushroom tyrosinase. *J Enzyme Inhib Med Chem* **21**: 711–717.
- Sanchez-Cortes S, Vasina M, Francioso O, Garcia-Ramos JV (1998) Raman and surface enhanced Raman spectroscopy of dithiocarbamate fungicides. *Vib Spectrosc* **17**: 133–144.
- Seo SY, Sharma VK, Sharma N (2003) Mushroom tyrosinase: recent prospects. *J Agric Food Chem* **51**: 2837–2853.
- Siddiqi KS, Sadaf K, Shahab AAN, El-ajaily MM (2007) Polynuclear transition metal complexes with thiocarbonylhydrazide and dithiocarbamates. *Spectrochim Acta Part A* **67**: 995–1002.
- Strothkamp KG, Jolley RL, Mason HS (1976) Quaternary structure of mushroom tyrosinase. *Biochem Biophys Res Commun* **70**: 519–524.
- Vaneeet KS, Aulakh SJ, Malik AK (2005) Fourth derivative spectrophotometric determination of fungicide thiram (tetramethyldithiocarbamate) using sodium molybdate and its application. *Talanta* **65**: 375–379.